Available online at www.sciencedirect.com
SCIENCE DIRECT®
Surface Science 523 (2003) 48–58
SURFACE SCIENCE
www.elsevier.com/locate/susc

Vibrational electron energy loss studies of surface processes on Si(1 1 1)7 × 7 and vitreous SiO_2 ion-mediated in CF_4 and CH_2F_2

Zhenhua He, K.T. Leung *

Department of Chemistry, University of Waterloo, Waterloo, Ont., Canada N2L 3G1

Received 19 June 2002; accepted for publication 17 September 2002

Abstract

The surface species produced on Si(1 1 1)7 × 7 and vitreous SiO_2 surfaces by ion irradiation in CF_4 and in CH_2F_2 at 50 eV impact energy have been investigated by electron energy loss spectroscopy (EELS), thermal desorption spectrometry (TDS) and low energy electron diffraction (LEED). In particular, the reaction layer for Si(1 1 1)7 × 7 ion-irradiated in CF_4 is characterized by the presence of Si–C stretching, Si–F_x ($x = 1$–3) stretching and bending modes, while ion irradiation in CH_2F_2 introduces additional C–H stretching mode. For both cases, the absence of C–F stretching feature in the corresponding EELS spectra indicates that CF_x ($x = 1$–3) surface species do not present in any appreciable amount. These EELS results are consistent with the TDS data, which shows that SiF_4 is the major desorption product and desorption products such as CF_x ($x = 1$–3) are not observed. Ion irradiation of Si(1 1 1)7 × 7 in CF_4 or CH_2F_2 at low impact energy therefore produces SiC and SiF_x ($x = 1$–3) as the primary surface products, while additional CH species is found in the latter case of ion-irradiation in CH_2F_2. When the oxidized surface instead of the 7 × 7 surface of Si(1 1 1) is used as the substrate, ion irradiation by the same dose of fluorocarbon ions appears to enhance the deposition of SiF_x but reduce the amount of SiC species, which provides evidence for recombination reaction of surface O with surface C to form gaseous CO or CO_2, leaving behind more F to interact with the Si substrate atoms. The corresponding TDS data suggests that the OCF radical may also be one of the minor desorption products.

Keywords: Ion bombardment; Chemisorption; Electron energy loss spectroscopy (EELS); Silicon; Silicon oxides; Halides

1. Introduction

The deposition of fluorocarbon films under appropriate plasma conditions and its subsequent effects on directional etching on silicon substrate has been the subject of intense investigation [1–4]. In particular, the energetics of the ions appears to play an important role in plasma–substrate interactions and the associated surface chemistry [5]. Together with other plasma conditions, the ion energetics can also shift the equilibrium between the deposition and etching regimes. Furthermore, manipulation of the kinematics (flux, kinetic energy, etc.) of the ions and radicals in the plasma could lead to desirable gas-phase polymerization

* Corresponding author. Tel.: +1-519-8884567x5826; fax: +1-519-7460435.
E-mail address: tong@uwaterloo.ca (K.T. Leung).

0039-6028/02/$ - see front matter
PII: S0039-6028(02)02351-8

for deposition of polymer films [1]. A balance between etching and polymerization has been shown to depend on the F-to-C ratio of the precursor of the plasma [6]. Some attempts to understand the mechanisms of plasma-mediated processes have been made under simplified conditions using XeF_2 and F_2 [5,7]. Mass-separated low-energy molecular ion beams have been used to study specific ion-mediated surface processes [8], and the effects of ion bombardment on the reaction layer under realistic plasma conditions have been investigated [9]. Since manufacturing of modern microelectronic devices often involves such key steps as selective etching of SiO_2 over Si with a high aspect ratio, a better understanding of the complex plasma chemistry and its effects on the substrate would be of great interest.

In the case of fluorocarbon plasma etching of Si or SiO_2, the formation of a thin fluorocarbon or fluorinated silicon oxide (SiOF) reaction layer has been observed [10]. Along with fluoropolymer, fluorinated amorphous carbon and fluorocarbonated SiO_2 films, SiOF films have attracted a lot of recent attention because of their low dielectric constant, which makes them viable candidates as a new type of inter-metal dielectric materials for microelectronic applications. In particular, the incorporation of fluorine into these materials changes the Si–O network to a less polarizable geometry, reducing the dielectric constant. The formation of these fluorocarbonated SiO_2 films is usually achieved by plasma enhanced chemical vapour deposition [10]. A better understanding of the fluorocarbon–surface interaction may provide new insight into the early stage of formation and the subsequent reactions of this type of films. In spite of the extensive studies on the effects of ion bombardment on silicon [7–9,11], the interactions of fluorocarbon ions with Si remain poorly understood, especially for bombardment energy below 100 eV. Many surface diagnostic tools including X-ray photoelectron spectroscopy, Auger electron spectroscopy (AES), and Fourier transform infrared spectroscopy have been used to investigate the surface processes induced by ion irradiation of halocarbons [8,12–15]. Recently, we have investigated the surface products on clean and oxidized surfaces of Si(1 1 1)7×7 generated by ion irradiation in CF_4 at 50 eV impact energy by using the more surface-sensitive vibrational EELS technique [16]. We now extend this EELS study to ion irradiation in CH_2F_2 in order to examine the role of the F-to-C ratio of the medium gas in controlling the types of surface species so produced and the corresponding ion-mediated processes.

2. Experimental

The experimental apparatus used in the present work has been described in detail elsewhere [17]. All the experiments were performed in a home-built ultra-high vacuum chamber with a base pressure better than 1×10^{-10} Torr, which was equipped with an ion (-sputtering) gun, a four-grid retarding-field optics for both reverse-view LEED and AES, a differentially pumped 1–300 amu quadrupole mass spectrometer for TDS studies, and a home-built multi-technique electron spectrometer for both electronic and vibrational EELS measurements. Details of our EELS spectrometer have been given in Ref. [18]. All of the present EELS measurements were conducted with the sample held at room temperature (RT) under specular reflection scattering condition of 45° from the surface normal [17,18]. It should be noted that in the present vibrational EELS study involving Si surfaces irradiated by low-energy ions, the surface roughness generally reduced the obtainable energy resolution and count rate. Despite this inherent challenge, a routine energy resolution of 15–22 meV (120–180 cm^{-1}) full-width at half-maximum (FWHM) could be achieved with our spectrometer at 5 eV impact energy with a typical count rate of 100,000 counts per second for the elastic peak.

The Si(1 1 1) sample (p-type boron doped, 50 Ωcm, 8×6 $mm^2 \times 0.5$ mm thick) with a stated purity of 99.999% was purchased from Virginia Semiconductor Inc. The sample was mechanically fastened to a Ta sample plate with 0.25-mm-diameter Ta wires and could be annealed by electron bombardment from a heated tungsten filament at the backside of the sample. The Si(1 1 1) sample was cleaned by using a standard procedure

involving repeated cycles of Ar^+ sputtering and annealing to 1200 K until a sharp 7×7 LEED pattern was observed. The cleanliness of the sample was further verified in situ by the lack of any detectable vibrational EELS feature attributable to unwanted contaminants, particularly the Si–C stretching mode at 800–850 cm^{-1}. The sensitivity of this Si–C feature as an indicator of surface cleanliness was found to be far superior to that achievable by AES using our LEED optics (5% at best). The gaseous samples, carbon tetrafluoride (CF_4, at 99.9% purity) and difluoromethane (CH_2F_2, at 99.7% purity), were obtained from Aldrich, while oxygen (at 99.99% purity) was purchased from Matheson. All the gaseous samples were used without further purification.

Ion irradiation was performed on a sample positioned 5 cm from the front face of the ion gun, by operating the ion gun with the chamber backfilled with the medium gas of interest to a working pressure of 2×10^{-5} Torr. The impact energy of the ion beam could be controlled by adjusting a floating voltage applied on the sample with respect to a pre-selected beam energy of the ion gun. The ion dose can be estimated by the product of the ion flux (estimated to be $\sim$2 nA/mm^2) and the exposure time (obtained from the exposure in units of Langmuir ($1\ L = 1 \times 10^{-6}$ Torr s) and the working pressure). Inside the ion gun, the medium gas was ionized by electrons with 180 eV kinetic energy, and only positive ions from the ion gun could reach the sample without mass selection. The concentration of each ion can be estimated from the cracking pattern of the corresponding molecule reported in the literature [19,20]. In the case of CF_4, CF_3^+ is the majority or base ion (estimated to be 78%), with other smaller ions such as CF_2^+ (10%) and CF^+ (3%) present at lower concentrations [21]. For CH_2F_2, CH_2F^+ (38%) and CHF_2^+ (37%) are the majority ions, while CF^+ (11%), CHF^+ (4%), CH_2F^+ (3.8%), CH^+ (2%), and CF_2^+ (1%) are the minority ions [20]. When the ions collide with the surface, they may become neutralized and/or undergo further dissociation into other smaller fragments including C and F atoms. The resulting fragments and radicals may subsequently react with the substrate atoms and/or other pre-deposited surface species.

3. Results and discussion

3.1. EELS spectra of ion irradiation of Si(1 1 1)7 × 7 in CF_4 and in CH_2F_2

The vibrational EELS spectra of Si(1 1 1)7×7 ion-irradiated in CF_4 at 50 eV impact energy as a function of exposure at RT (shown in Fig. 1) are compared with the corresponding spectra for ion irradiation in CH_2F_2 (shown in Fig. 2). In the case of ion irradiation in CF_4 (Fig. 1), only one prominent EELS feature at 780 cm^{-1} is observed at 1 kL (1 kL = 1000 L) and it appears to blueshift with increasing ion exposure gradually to 885 cm^{-1} at 10 kL (Fig. 1d). A weak feature at 340 cm^{-1} emerges as a shoulder at 2.5 kL (Fig. 1b) and becomes a well-defined peak at higher exposure (10 kL, Fig. 1d). To facilitate spectral assignments in this work, we have summarized in Table 1 reference infrared spectroscopic data for common inorganic materials reported in the literature [22–29]. In particular, the Si–C stretching mode is

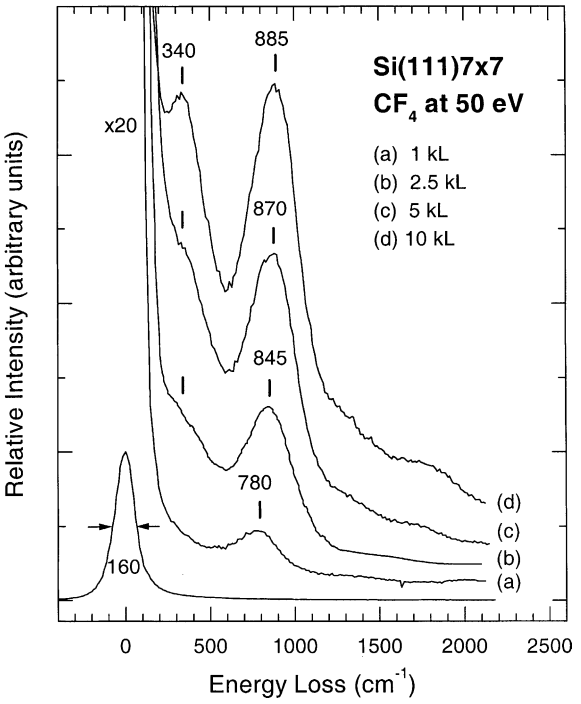

Fig. 1. Vibrational electron energy loss spectra for Si(1 1 1)7×7 ion-irradiated at 50 eV impact energy in (a) 1 kL, (b) 2.5 kL, (c) 5 kL, and (d) 10 kL of CF_4.

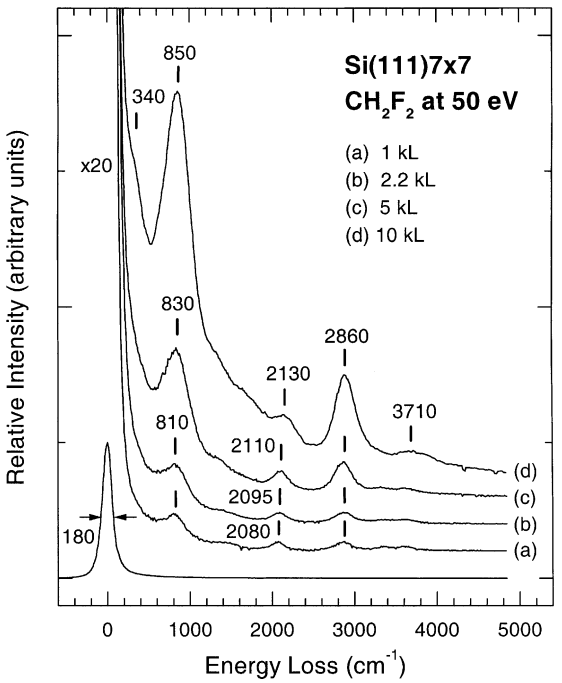

Fig. 2. Vibrational electron energy loss spectra for Si(1 1 1)7 × 7 ion-irradiated at 50 eV impact energy in (a) 1 kL, (b) 2.2 kL, (c) 5 kL, and (d) 10 kL of CH_2F_2.

commonly observed at 750–950 cm^{-1} [26,27] while the Si–F stretching mode usually occurs at 825–850 cm^{-1}. For Si–F_x ($x = 2$–3) species, the bending (rocking vibration), symmetric and asymmetric stretching modes are generally found at 300–380, 827–870 and 920–1015 cm^{-1}, respectively [22–25]. Table 1 therefore suggests that the broad lower energy-loss feature at 340 cm^{-1} can be assigned as the Si–F_x ($x = 1$–3) bending mode, while the higher energy-loss feature at 780–885 cm^{-1} can be attributed to a combination of Si–C and Si–F_x ($x = 1$–3) stretching modes.

In the case of Si(1 1 1)7 × 7 ion-irradiated in CH_2F_2 (Fig. 2), similar coverage dependence can be found for the lower-energy features at 340 and 810–850 cm^{-1}. In addition, two new features can be observed at 2080–2130 and 2860 cm^{-1} for all the exposures, with the feature at 2860 cm^{-1} apparently becoming more intense with increasing ion exposure than that at 2080–2130 cm^{-1}. The features at 2080–2130 and 2860 cm^{-1} for the case of CH_2F_2 ion irradiation correspond, respectively, to the well-known Si–H [28] and the C–H stretching modes of adsorbed hydrocarbon species. The presence of these features therefore suggests that H, F and CH are the primary surface products on Si(1 1 1)7 × 7 upon ion irradiation in CH_2F_2 at 50 eV impact energy.

The ion exposure dependence data therefore shows that SiC and SiF_x are the predominant

Table 1
Vibrational frequencies (in cm^{-1}) of reference silicon and related systems

Vibrational mode	This work	Ref. [24]	Ref. [25]	Refs. [26–29]
Si–F bend	340	300		
Si–F_2 bend	340	300		
Si–F_3 bend	340	337		
Si–F_4 bend			380	
Si–C stretch	810–850			750–950
Si–F stretch	780–885	850	825	
Si–F_2 stretch	780–885	827[a], 870[a], 920[b], 965[b]	920	
Si–F_3 stretch	780–885	838[a], 1015[b]	965	
Si–H stretch	2080–2180			2088–2120
C–H stretch	2860			2860–3000
C–H_2 stretch				2879–2955
C–H_3 stretch				2879–2955
O–H stretch	3670			3680–3700
Si–OH bend				800–820
Si–O–Si rock	385			350–480
Si–O–Si stretch	710[a], 1040[b]			690–840[a], 1050–1180[b]

[a] Symmetric stretch.
[b] Asymmetric stretch.

products on Si(1 1 1)7 × 7 as a result of ion irradiation with increasing CF_4 or CH_2F_2 exposure. In the case of SiF_x, the lack of a bending mode (the energy loss feature at 340 cm^{-1}) suggests that only SiF is formed at low exposure (1 kL). At higher exposure, the emergence of the bending mode at 340 cm^{-1} provides evidence for the formation of SiF_2 and SiF_3 surface species. However, the barely visible shoulder at 340 cm^{-1} in the case of CH_2F_2 ion irradiation at higher exposure suggests that the formation of these larger SiF_x ($x = 2$–3) species even at 10 kL is not prominent (Fig. 2d). The blue shift of the higher energy feature from 780 to 885 cm^{-1} with increasing CF_4 ions exposure (Fig. 1) is also consistent with the increasing contributions from the Si–F_x symmetric and asymmetric stretching modes of the larger fluorocarbon species (SiF_2 and SiF_3) that occur at higher energy losses. There is a smaller blue shift (from 810 to 850 cm^{-1}) in the case of CH_2F_2 ion irradiation (Fig. 2) with respect to the CF_4 ion irradiation case, which is consistent with the smaller moiety for the larger SiF_x ($x = 2$–3) species (as reflected also by the very weak SiF_x bending feature at 340 cm^{-1}). This difference in the SiF_x moiety at higher exposure may be related to the F-to-C ratio of the medium gases (4 for CF_4 and 2 for CH_2F_2).

The lack of any prominent feature at ~1024 cm^{-1}, commonly attributable to C–F stretching modes [30], for ion irradiation in CF_4 or CH_2F_2 suggests that fluorocarbon (CF_x ($x = 1$–3)) species are not among the surface products. This result is in good accord with the earlier work reported by Winters and Coburn [5], which showed that most of the CF_x^+ ions completely dissociate into C and F atoms upon impact with the Si surface. Chemisorption of the resulting C and F atoms on the Si substrate leads to the formation of SiC and various SiF_x species with the characteristic energy loss features mentioned above. The nature of this type of "disordered" SiC surface species has been examined in more detail by other techniques (including electronic EELS and AES) in our earlier work [34], and these SiC species are believed to involve Si–C bonds not necessarily fully terminated. In the case of ion irradiation in CH_2F_2, the presence of hydrocarbon species as one of the predominant products (in addition to SiC and SiF_x) is clearly evident, as indicated by the C–H stretch at 2860 cm^{-1} (Fig. 2). The CH species likely come from fragments of the impinging ions such as CH_2F^+ and CHF_2^+. It is of interest to note that Sugai et al. [31] also observed fragmentation of hydrocarbon ions CH_x^+ ($x = 1$–4), unlike fluorocarbon ions CF_x^+ ($x = 1$–3), which hardly break up into smaller fragment ions, on impact with an Al substrate at 10–50 eV impact energy. The difference, however, may be due to the larger Si–F affinity relative to the C–F affinity (with a generally larger bond strength for Si–F than for C–F bond).

The effects of annealing the resulting surface species obtained by ion-irradiation of Si(1 1 1)7 × 7 in a large exposure of CF_4 (Fig. 1d) and of CH_2F_2 (Fig. 2d) are shown in Figs. 3 and 4, respectively. In particular, annealing the Si(1 1 1)7 × 7 sample ion-irradiated in CF_4 (Fig. 3a) to 700 K is sufficient to remove the Si–F_x bending features at

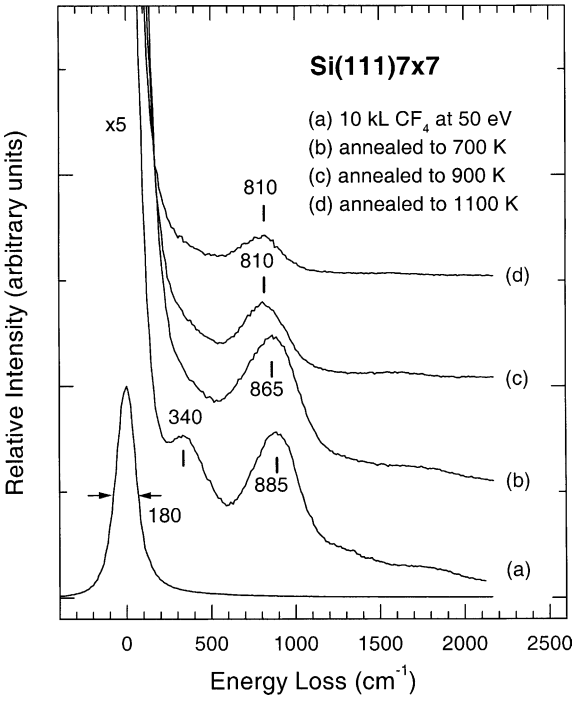

Fig. 3. Vibrational electron energy loss spectra for Si(1 1 1)7 × 7 ion-irradiated at 50 eV impact energy in (a) 10 kL of CF_4, followed by annealing to (b) 700 K, (c) 900 K, and (d) 1100 K.

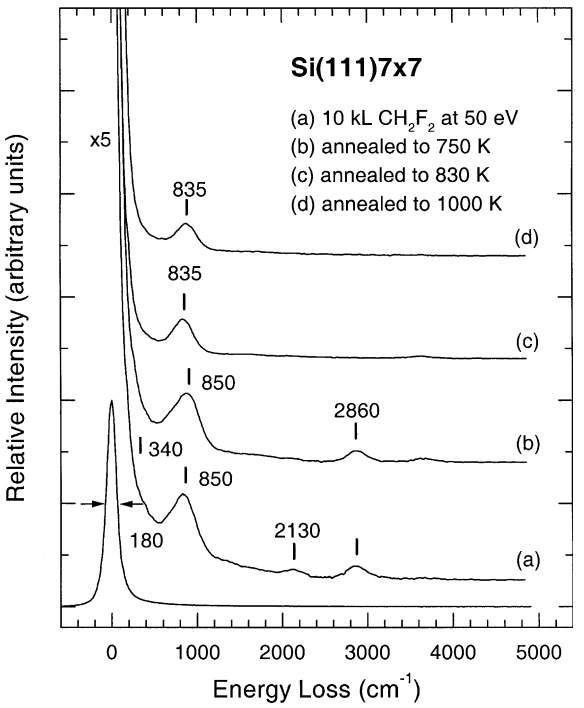

Fig. 4. Vibrational electron energy loss spectra for Si(1 1 1)7 × 7 ion-irradiated at 50 eV impact energy in (a) 10 kL of CH_2F_2, followed by annealing to (b) 750 K, (c) 830 K, and (d) 1000 K.

340 cm^{-1} (Fig. 3b), which indicates desorption of the larger SiF_2 and SiF_3 species from the surface. Further successive annealing to higher temperature not only reduces the intensity of the broad peak at 885 cm^{-1} but also causes it to red-shift back to a lower frequency of 810 cm^{-1} (characteristic of the Si–C stretching mode), as shown in Fig. 3c. Similar general changes to the feature(s) at 850 cm^{-1} (and 340 cm^{-1}) in the EELS spectrum with increasing annealing temperature are observed for the sample ion irradiated in 10 kL of CH_2F_2 (Fig. 4a). In good accord with the temperature behaviour of SiH species reported in the literature [32,33], the Si–H feature at 2130 cm^{-1} is completely removed above the recombinative desorption temperature of H_2 at 750 K (Fig. 4b). Further annealing the sample above 830 K completely depleted the remaining hydrogen-related feature, C–H stretch at 2860 cm^{-1} (Fig. 4c). These changes with increasing annealing temperature in turn reaffirm our spectral assignment of these H-related features.

The changes in the LEED pattern of the Si sample have also been monitored during the annealing experiment and these changes are found to be similar for ion irradiation in CF_4 or CH_2F_2. Ion irradiation of a clean Si(1 1 1)7 × 7 surface with 1–5 kL of CF_4 (Fig. 1a–c) or CH_2F_2 (Fig. 2a–c) at 50 eV impact energy caused the 7 × 7 LEED pattern to become a 1 × 1 pattern, which then reverted back to a weak and diffuse 7 × 7 pattern after the sample was annealed to 900 K. In contrast, ion irradiation with a heavier dose (10 kL) of CF_4 or CH_2F_2 at 50 eV impact energy (Fig. 3a or 4a) resulted in no discernible LEED pattern, which became a weak 1 × 1 and then a diffuse 7 × 7 pattern upon annealing to 900 and 1000 K, respectively. These changes in the TDS and LEED results are consistent with the model of continual desorption of SiF (and additional CH species in the case of CH_2F_2) from the surface, leaving SiC as the predominant surface product above 900 K (Fig. 3d or 4d).

3.2. EELS spectra of ion irradiation of vitreous SiO_2 surface in CF_4 and in CH_2F_2

Unlike the native oxide layer formed at RT, which has essentially the same Si–Si separation as that in crystalline silicon (2.35 Å), the vitreous SiO_2 in silica has a considerably larger Si–Si separation of 3.05 Å. The SiO_2 layer formed at RT has a more "compressed" structure with a smaller angle between the two Si–O bonds than the vitreous SiO_2, which can be obtained by annealing the sample after and/or during oxidization to 700 K or by ion bombarding the sample in O_2 at RT [34]. We believe that sputtering in other gases in the presence of native surface oxide can also induce the formation of vitreous SiO_2 at RT due to the breakage of the Si–Si back bonds caused by the sputtering process. The vitreous SiO_2 can be distinguished from the native SiO_2 formed at RT by the characteristic blue-shifts of approximately 10–130 cm^{-1} in their vibrational features from those of the native SiO_2 [29]. Following Ibach et al. [28], we prepared a vitreous SiO_2 layer by dosing 10 kL of O_2 to a Si(1 1 1)7 × 7 sample held at 700 K,

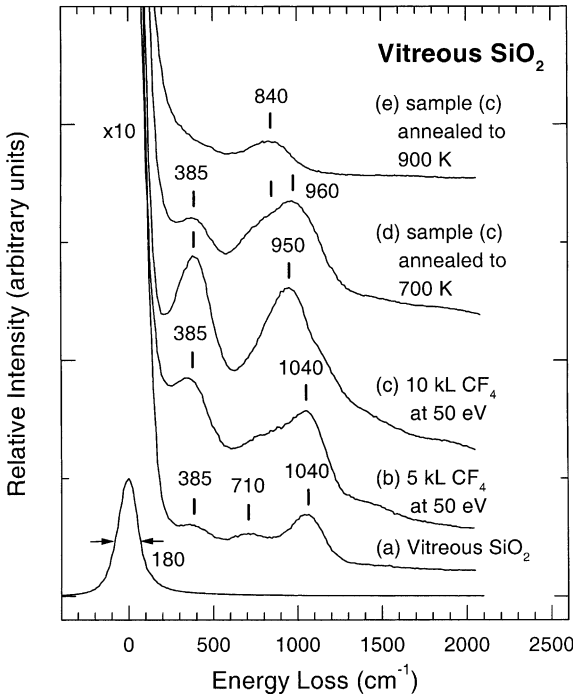

Fig. 5. Vibrational electron energy loss spectra for (a) vitreous SiO_2 and sample (a) ion-irradiated at 50 eV impact energy in (b) 5 kL and (c) 10 kL of CF_4, followed by annealing to (d) 700 K and (e) 900 K. The vitreous SiO_2 surface was obtained by exposing Si(1 1 1)7 × 7 to 10 kL of O_2 at 700 K.

which exhibited a weak 1 × 1 LEED pattern. As shown in Fig. 5a, such a vitreous SiO_2 surface is characterized by three energy loss features at 385, 710 and 1040 cm^{-1}, corresponding to respectively rocking (350–480 cm^{-1}), symmetric (690–840 cm^{-1}) and asymmetric stretching modes (1050–1180 cm^{-1}) of the Si–O–Si radical [29]. This relatively thick oxidized layer was prepared in order to study the reaction of fluorocarbon ions with surface oxygen in excess.

Fig. 5 illustrates the effects of ion irradiation in CF_4 at 50 eV impact energy on a vitreous SiO_2 surface. After ion irradiation of the oxidized surface with increasing exposure of CF_4 (5 kL in Fig. 5b and 10 kL in Fig. 5c), the three characteristic energy loss features of vitreous SiO_2 have evolved into a well-defined peak at 385 cm^{-1} attributable to Si–F_x bending modes, and a single broad band at 950 cm^{-1}, which can be assigned as a combination of the Si–O–Si stretching modes and the Si–C and Si–F_x stretching modes observed earlier (Fig. 1d). Evidently, the Si–F_x bending feature becomes more intense and appears at a higher energy loss (385 cm^{-1}) on the oxidized Si surface (Fig. 5c) relative to that of the 7 × 7 surface (Fig. 1d), which shows that a greater amount of the larger SiF_x ($x = 2$–3) species is produced on the vitreous SiO_2 surface. The presence of oxygen on the oxidized surface facilitates the removal of carbon on the surface and is believed to be responsible for opening up additional binding sites for surface F atoms. Furthermore, the blue shift of 65 cm^{-1} observed in the higher energy loss feature for the SiO_2 surface (950 cm^{-1}, Fig. 5c) relative to the 7 × 7 surface (885 cm^{-1}, Fig. 1d) could be attributed to the coupling of Si–O_x ($x = 1, 2$) vibrations to the existing Si–C and Si–F_x stretching modes [35].

Annealing the sample depicted in Fig. 5c to 700 K evidently reduces the feature at 385 cm^{-1} and introduces an apparent energy loss feature near 840 cm^{-1}, which can be attributed as before to the changes in the relative concentrations of Si–C and Si–F_x stretching modes (Fig. 5d). The considerable change in the relative intensity of the feature at 385 cm^{-1} clearly reflects the additional contribution from the Si–F_x bending modes (Fig. 5c) to the existing Si–O–Si rocking feature of the vitreous SiO_2 surface (Fig. 5a). Annealing the oxidized sample to 700 K therefore appears to consolidate the formation of an overlayer composed predominantly of SiC and SiF_x ($x = 1$–3) surface species. The disappearance of the low energy loss feature at higher annealing temperature is consistent with the earlier observation that the larger fluorosilicon (SiF_2 and SiF_3) surface species desorb above 700 K (Fig. 5d). Further annealing the oxidized sample above 900 K would desorb SiF species from the surface leaving behind only SiC species, which is consistent with the red shift of the higher energy loss feature back to 840 cm^{-1} (characteristic of the Si–C stretching mode, Fig. 5e). The higher energy loss position of the Si–C feature (at 840 cm^{-1}) for the vitreous SiO_2 surface (Fig. 5e) relative to that of the 7 × 7 sample (Fig. 1c) is likely caused by the presence of co-adsorbate interactions. Similar co-adsorbate-induced effects have also been observed in other systems including CO/Cu(1 0 0) [18].

Furthermore, the weaker Si–C feature for the oxidized sample suggests that the availability of O on the vitreous SiO_2 surface facilitates recombinative reactions with surface C to form gaseous CO and/or CO_2 and thus enhances the removal of both surface carbon (reducing the corresponding Si–C peak) and surface oxide.

Similar changes in the low energy loss region of the EELS spectrum can be observed for a vitreous SiO_2 surface ion-irradiated in CH_2F_2 at 50 eV impact energy. Fig. 6a shows the characteristic energy loss features at 385, 710, and 1040 cm^{-1}, corresponding, respectively, to rocking, symmetric and asymmetric stretching mode of the Si–O–Si structure. It should be noted that due to the surface roughness of the ion-irradiated samples (that generally contributes to a lower energy resolution), the reproducibility of the measured energy loss positions is limited to 2–4 meV (or 16–32 cm^{-1}) in the present work. A minute amount of water contamination on the vitreous SiO_2 surface is evident by the presence of the weak feature at 3670 cm^{-1}, characteristic of the O–H stretching mode. It should be noted that the Si–H stretching mode observed in Fig. 6 evidently occurs at a slightly higher energy loss (2180 cm^{-1}) than the corresponding feature (2130 cm^{-1}) in Fig. 4. This shift could be caused by the change in the electronegativity of the Si atoms due to the presence of oxygen as their neighbours [28,36]. As with ion irradiation in CF_4, increasing the ion-irradiation exposure in CH_2F_2 produces a similar change in the EELS spectrum below 1500 cm^{-1}. In particular, the Si–F_x bending modes at 385 cm^{-1} (Fig. 6a) become a shoulder for the 10 kL exposure (Fig. 6d) instead of a well-defined peak as for the CF_4 case shown in Fig. 5c, which suggests a smaller relative contribution from the larger SiF_x ($x = 2$–3) species due to the smaller F moiety in CH_2F_2. Furthermore, the Si–O–Si stretching modes at 710 and 1040 cm^{-1} evidently merge into a single broad band at 920 cm^{-1} (Fig. 6d), which can be attributed to a combination of Si–C and Si–F_x stretching modes observed earlier (Fig. 5). In the energy loss region above 1500 cm^{-1}, both the Si–H stretching at 2180 cm^{-1} and the C–H stretching mode at 2860 cm^{-1} strengthen continuously even at the 10 kL ion-irradiation exposure. Possible fragments such as CH_2F^+ and CHF_2^+ ions could atomize upon impact with the substrate, thereby increasing the moiety of atomic C and H on the surface and the corresponding intensities of the observed Si–H and C–H features. The ion exposure dependence of these features on the vitreous SiO_2 surface (Fig. 6) is found to be similar to that of the corresponding features for the 7×7 surface (Fig. 2).

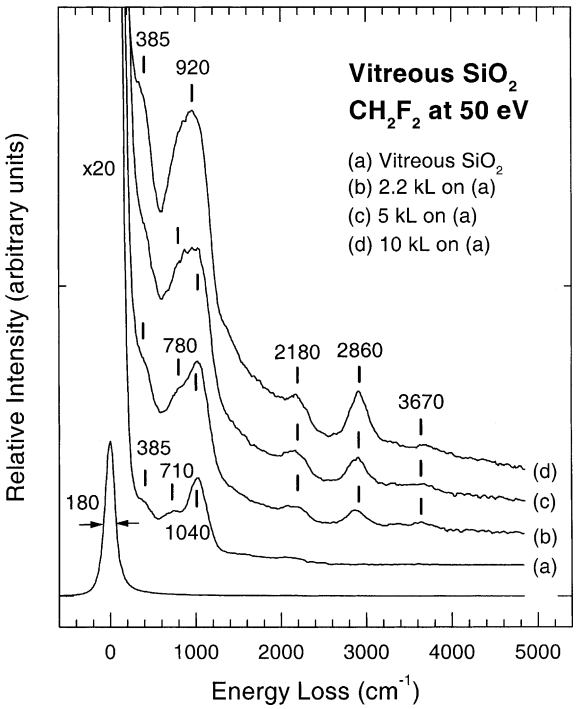

Fig. 6. Vibrational electron energy loss spectra for (a) vitreous SiO_2, and sample (a) ion-irradiated at 50 eV impact energy in (b) 2.2 kL, (c) 5 kL, and (d) 10 kL of CH_2F_2. The vitreous SiO_2 surface was obtained by exposing Si(1 1 1)7×7 to 10 kL of O_2 at 700 K.

Fig. 7 depicts the effect of annealing a vitreous SiO_2 sample ion-irradiated with 10 kL of CH_2F_2 at 50 eV impact energy (Fig. 6d). Annealing the sample to 780 K (Fig. 7d) appears to remove most of the surface species, reverting the surface to an essentially pre-ion-irradiation state (cf. Fig. 7a). In particular, the three characteristic Si–O–Si vibrational features in the energy loss region below 1500 cm^{-1} have become generally sharper, while the Si–H (2180 cm^{-1}) and C–H (2860 cm^{-1}) features have

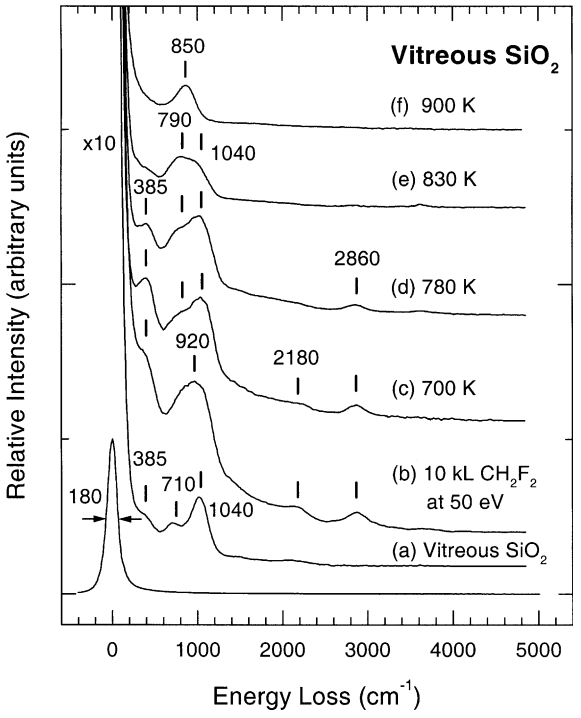

Fig. 7. Vibrational electron energy loss spectra for (a) vitreous SiO_2, and (b) sample (a) ion-irradiated at 50 eV impact energy in 10 kL of CH_2F_2, followed by annealing to (c) 700 K, (d) 780 K, (e) 830 K, and (f) 900 K. The vitreous SiO_2 surface was obtained by exposing Si(1 1 1)7 × 7 to 10 kL of O_2 at 700 K.

become less intense with successive annealing to higher temperature. Above the annealing temperature of 700 K, the Si–H stretching feature at 2180 cm^{-1} is essentially removed (Fig. 7d), which indicates breakage of the Si–H bonds leading to recombinative desorption of surface H [32]. Similar dissociation of the surface CH species (or desorption of CH species) proceeds to completion at an annealing temperature greater than 780 K, as indicated in Fig. 7e by the complete disappearance of the C–H stretching mode at 2860 cm^{-1}. Annealing the sample to 830 K (Fig. 7e) also reduces all the Si–O–Si modes, most notably the modes at 385 and 1040 cm^{-1}, revealing the broad feature at 790 cm^{-1}. Further annealing to 900 K (Fig. 7f) produces a single sharp feature at 850 cm^{-1}, which could be assigned as a Si–C stretching mode.

For the vitreous SiO_2 surface, the changes in the EELS spectrum and the associated surface species for ion irradiation in CH_2F_2 as a function of the annealing temperature (Fig. 7) are therefore quite similar to those for ion irradiation in CF_4 (Fig. 5). The dramatic changes in the EELS spectra for the vitreous SiO_2 sample suggest that low-energy ion irradiation in CF_4 or CH_2F_2 followed by annealing could provide an efficient way of removing surface oxides.

3.3. TDS profiles for ion irradiation of Si(1 1 1)7 × 7 and vitreous SiO_2 in CF_4 and in CH_2F_2

Fig. 8 compares the TDS profiles of mass 85 (SiF_3^+), mass 66 (SiF_2^+), and mass 47 (SiF^+) for the Si(1 1 1)7 × 7 and vitreous SiO_2 surfaces after ion irradiation in 10 kL of CF_4 at 50 eV impact energy with the corresponding profiles for ion irradiation in 10 kL of CH_2F_2. Given that the gas-phase cracking pattern of SiF_4 reveals SiF_3^+ as the pre-

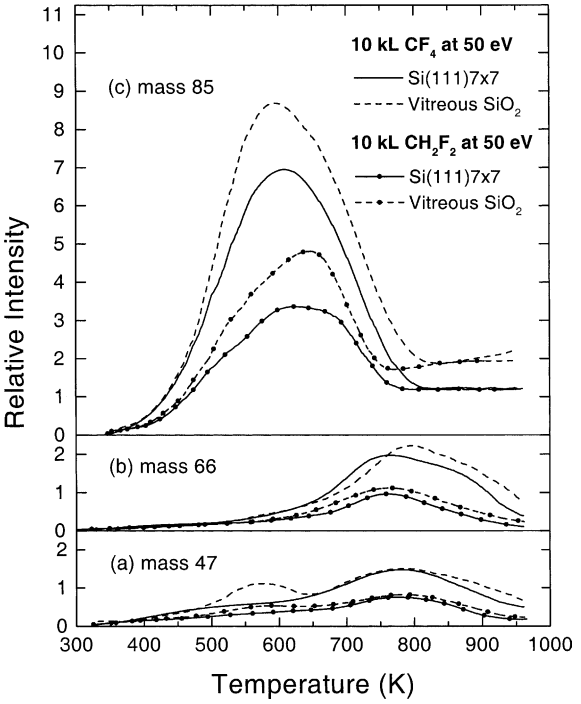

Fig. 8. Thermal desorption profiles of (a) mass 47 (SiF^+ or OCF^+), (b) mass 66 (SiF_2^+), and (c) mass 85 (SiF_3^+) for Si(1 1 1)7 × 7 and vitreous SiO_2. The vitreous SiO_2 surface was obtained by exposing Si(1 1 1)7 × 7 to 10 kL of O_2 at 700 K.

dominant (90%) ion (base mass) [21], the large desorption intensity found for mass 85 for a set of TDS profiles of a particular sample (e.g., Si(1 1 1)7 × 7 ion-irradiated in CF_4) therefore indicates that SiF_4 is the major desorption product. The corresponding TDS profile of SiF_2^+ (mass 66) is found to be essentially identical to that of SiF^+ (mass 47), with a prominent desorption band at ~780 K, indicating that both ions originate from the same parent species. Because SiF_2^+ and SiF^+ are found in comparable amounts from electron impact ionization of gaseous SiF_2 [5,37], the parent species is most likely SiF_2. Furthermore, the TDS profiles for both SiF_2^+ (mass 66) and SiF^+ (mass 47) for the same sample clearly have a different desorption maximum than that for SiF_3^+ (mass 85), which is consistent with the hypothesis that these two ions originate from a different desorption product (SiF_2). Our TDS results are found to be in general accord with the results for gas-phase reaction products (SiF, SiF_2 and SiF_4 species) generated by other means, as reported by Winters and Coburn [5] and Engstrom et al. [38]. We also monitored fluorocarbon fragments, including mass 69 (CF_3^+), mass 50 (CF_2^+) and mass 31 (CF^+), during the TDS experiments. The lack of any desorption feature for these masses confirms that no substantial amount of CF_x species is present (or formed during thermal desorption) on the Si(1 1 1)7 × 7 or vitreous SiO_2 surface as a result of ion irradiation in CF_4 or CH_2F_2.

Fig. 8 also shows that the TDS profiles of the respective masses for both the Si(1 1 1)7 × 7 and vitreous SiO_2 surfaces ion-irradiated in either fluorocarbon (CF_4 or CH_2F_2) are very similar to each other. Despite the similarity, the TDS profile of mass 47 for the oxidized surface exhibits an additional desorption peak at 580 K. Since the base mass for OCF_2 corresponds to OCF^+ [20], which has the same mass 47 as SiF^+, the new TDS feature near 580 K could be due to OCF^+. However, given that there is no corresponding desorption feature at 580 K for mass 66, which is the parent mass of OCF_2^+, the formation of OCF radical (instead of OCF_2) is therefore more likely. This result suggests that unlike the 7 × 7 surface, the presence of oxygen on the oxidized Si surface after ion irradiation in CF_4 or CH_2F_2 makes possible recombinative desorption of surface O, (Si–)C, and (Si–)F, making OCF a plausible desorption product.

Finally, there are striking similarities between the TDS profiles of the respective masses for either Si(1 1 1)7 × 7 or vitreous SiO_2 ion-irradiated in CF_4 and the corresponding profiles for either surface ion-irradiated in CH_2F_2. The two sets of TDS profiles only differ from each other in their corresponding desorption intensities, with the desorption intensities for ion irradiation in CF_4 being almost twice of those for ion irradiation in CH_2F_2. Considering the fact that CF_4 contains twice as many F atoms as CH_2F_2, the amount of F or F-containing fragments produced by ion irradiation in CF_4 is expected to be also double that produced by ion irradiation in CH_2F_2, which could account for the observed intensity differences in the TDS profiles.

4. Summary

In the present work, we compare the surface processes on Si(1 1 1)7 × 7 and vitreous SiO_2 surfaces induced by ion irradiation in CF_4 and in CH_2F_2 at 50 eV impact energy. Our results reveal very similar behaviour for species produced by ion irradiation in either CF_4 or CH_2F_2 on these substrate surfaces. In particular, our vibrational EELS data shows that SiC and SiF_x ($x = 1$–3) are the primary surface species on both 7 × 7 and oxidized Si surfaces produced by ion irradiation in CF_4 and in CH_2F_2 at high exposure, while no evidence for the presence of CF_x species for these samples is found. For ion irradiation in CH_2F_2, additional H related species including SiH and CH could be observed. These products are consistent with the picture of substantial atomization of the impinging fluorocarbon ions into C, H and F on the surface, the interaction of which with either Si or O substrate atoms then leads to the observed surface vibrations. Along with our TDS experiments, these EELS spectra further show that there is more SiF_x but less SiC formed on the vitreous SiO_2 surface than Si(1 1 1)7 × 7 by ion irradiation with the same dose of fluorocarbon ions, which suggests that surface C species may combine with

surface O to form gaseous CO and/or CO_2, thus leaving a relatively higher F moiety to bind with the substrate Si atoms. The TDS results also suggest that OCF may be one of the minor desorption products for the oxidized surfaces ion-irradiated in either CF_4 or CH_2F_2. The intensity difference between the TDS products for ion irradiation in CF_4 and those for ion irradiation in CH_2F_2 is found to be consistent with the number of constituent F atoms in the aforementioned picture involving atomization of the incoming ions. Other studies conducted in our group show that the surface processes mediated by ion irradiation in CF_4 at low impact energy (50 eV) are qualitatively similar to those at a higher impact energy (500 eV). The present work thus illustrates some of the intricate fluorocarbon ion surface chemistry on common semiconductor materials.

Acknowledgements

This work was supported by the Natural Sciences and Engineering Research Council of Canada.

References

[1] G.S. Oehrlein, Surf. Sci. 386 (1997) 222.
[2] C.B. Labelle, K.K. Gleason, J. Vac. Sci. Technol. A 17 (1999) 445.
[3] R. d'Agostino, P. Capezzuto, G. Bruno, F. Cramarossa, Pure Appl. Chem. 57 (1985) 1287.
[4] T. Shirafuji, W.W. Stoffels, H. Moriguchi, K. Tachibana, J. Vac. Sci. Technol. A 15 (1997) 209, and references therein.
[5] H.F. Winters, J.W. Coburn, Surf. Sci. Rep. 14 (1992) 161.
[6] J.W. Coburn, H.F. Winters, J. Vac. Sci. Technol. 16 (1979) 391.
[7] J.W. Coburn, J. Vac. Sci. Technol. A 12 (1994) 1417.
[8] I. Bello, W.H. Chang, W.M. Lau, J. Vac. Sci. Technol. A 12 (1994) 1425;
W.H. Chang, I. Bello, W.M. Lau, J. Vac. Sci. Technol. A 11 (1993) 1221.
[9] G.S. Oehrlein, J. Vac. Sci. Technol. A 11 (1993) 34.
[10] K.S. Oh, M.S. Kang, K.M. Lee, D.S. Kim, C.K. Choi, S.M. Yun, H.Y. Chang, K.H. Kim, Thin Solid Films 345 (1999) 45.
[11] Y. Horiike, M. Shibagaki, K. Kadono, Jpn. J. Appl. Phys. 18 (1979) 2309.
[12] K. Miyake, S. Tachi, K. Yagi, T. Tokuyama, J. Appl. Phys. 53 (1982) 3214.
[13] D.J. Thomson, C.R. Helms, Appl. Phys. Lett. 46 (1985) 1103.
[14] G.S. Oehrlein, J.G. Clabes, P. Spirito, J. Electrochem. Soc. 133 (1986) 1002.
[15] S.W. Robey, G.S. Oehrlein, Surf. Sci. 210 (1989) 429.
[16] Z.-H. He, K.T. Leung, Appl. Surf. Sci. 174 (2001) 225.
[17] D.Q. Hu, Ph.D. Thesis, University of Waterloo, Waterloo, 1993.
[18] H. Yu, D.Q. Hu, K.T. Leung, J. Vac. Sci. Technol. A 15 (1997) 2653.
[19] Eight Peak Index of Mass Spectra, Mass Spectrometry Data Center, Aldermaston, vol. 1, 1974.
[20] NIST/EPA/NIH Mass Spectral Library, NIST'98 with Windows, Version 1.7 software, 1996.
[21] P.W. Harland, S. Cradock, J.C. Thyne, Int. J. Mass Spectrom. Ion Phys. 10 (1972/73) 169.
[22] K. Nakamoto, Infrared and Raman Spectra of Inorganic and Coordination Compounds, Wiley, New York, 1986, p. 132.
[23] L. Ley, H.R. Shanks, C.J. Fang, K.J. Gruntz, M. Cardona, J. Phys. Soc. Jpn., Suppl. A 49 (1980) 1241.
[24] T. Shimada, Y. Katayama, S. Horigome, Jpn. J. Appl. Phys. 19 (1980) L265;
T. Shimada, Y. Katayama, J. Phys. Soc. Jpn., Suppl. A 49 (1980) 1245.
[25] K. Yamamoto, M. Tsuji, K. Washio, H. Kasahara, K. Abe, J. Phys. Soc. Jpn. 52 (1983) 925.
[26] J. Yoshinobu, H. Tsuda, M. Onchi, M. Nishijma, J. Chem. Phys. 87 (1987) 7332.
[27] J. Schmidt, C. Stuhlmann, H. Ibach, Surf. Sci. 302 (1994) 10.
[28] H. Ibach, H. Wagner, D. Bruchmann, Solid State Commun. 42 (1982) 457.
[29] H. Ibach, H.D. Bruchmann, H. Wagner, Appl. Phys. A 29 (1982) 113.
[30] K. Nagai, C. Yamada, Y. Endo, E. Hirota, J. Mol. Spectrosc. 90 (1981) 249.
[31] H. Sugai, Y. Mitsuoka, H. Toyoda, J. Vac. Sci. Technol. A 16 (1998) 290.
[32] C.C. Cheng, P.A. Taylor, R.M. Wallace, H. Gutleben, L. Clemen, M.L. Colaianni, P.J. Chen, W.H. Weinberg, W.J. Choyke, J.T. Yates Jr., Thin Solid Films 225 (1993) 196.
[33] H. Froitzheim, U. Köhler, H. Lammering, Surf. Sci. 149 (1985) 537.
[34] H. Yu, K.T. Leung, Surf. Sci. 432 (1999) 245.
[35] S.M. Han, E.S. Aydil, J. Vac. Sci. Technol. A 15 (1997) 2893.
[36] J.A. Schaefer, F. Stucki, D.J. Frankel, W. Gopel, G.J. Lapeyre, J. Vac. Sci. Technol. B 2 (1984) 359.
[37] R.J. Shul, T.R. Hayes, R.C. Weitzel, F.R. Baicchi, R.S. Freund, J. Chem. Phys. 89 (1988) 4042.
[38] J.R. Engstrom, M.M. Nelson, T. Engel, Surf. Sci. 215 (1989) 437.